Microvesicles rleased from *Giardia intestinalis* disturb host-pathogen response in vitro.

Ingrid Evans-Osses[1], Andres Mojoli [1] , Marta Monguió-Tortajada [2] , Antonio Marcilla [3,4] Veronica Aran [5], Jameel Inal [6] ,Francesc E. Borràs [2,7] and Marcel I.Ramirez [1,8]

1- Fundacao Oswaldo Cruz-Instituto Oswaldo Cruz .Av Brasil 4365.Manguinhos, Rio de janeiro. Brazil

2-REMAR-IVECAT Group, Health Science Research Institute Germans Trias i Pujol, Can Ruti Campus, Badalona, Spain

3- Área de Parasitología, Departamento de Farmacia y Tecnología Farmacéutica y Parasitología, Universitat de València, Av. V.A. Estellés, s/n, 46100 Burjassot (Valencia), Spain.

4- Joint Research Unit on Endocrinology, Nutrition and Clinical Dietetics, Health Research Institute-La Fe, Universitat de Valencia, 46026 Valencia, Spain

5- Brazilian National Cancer Institute, Rio de Janeiro, Brazil

6-Cellular and Molecular Immunology Research Centre, School of Human Sciences, London Metropolitan University, London, U.K., N7 8DB.

7-Nephrology Service, Germans Trias i Pujol University Hospital, Badalona, Spain

8- Dpto de Bioquimica, Universidade Federal de Parana, Curitiba, PR, Brazil

Corresponding Author: Marcel I Ramirez Insitituto Oswaldo cruz -Fiocruz.Av Brasil 4365.Manguinhos, Rio de janeiro .Brazil/ Dpto de Bioquimica Universidade Federal de Parana, Curitiba, Parana, Brasil . e-mail marcelr@ioc.fiocruz.br

Keywords: Microvesicles, parasite-host cell interactions, innate immunity, diarrhoea, *Giardia intestinalis*, extracellular vesicles.

ABSTRACT

Giardia intestinalis (G.I), is an anaerobic protozoan and the aetiological agent of giardiasis, a diarrhoea present worldwide and associated with poverty. G.I has a simple life cycle alternating between cyst and trophozoite. Cysts are transmitted orally to the stomach and transform to trophozoites in the intestine by a multifactorial process. Recently, microvesicles (MVs) have been found to be released from a wide range of eukaryotic cells. We have observed a release of MVs during the life cycle of G.I., identifying MVs from active trophozoites and from trophozoites differentiating to the cyst form. The aim of the current work was to investigate the role of MVs from G.I in the pathogenesis of giardiasis. MVs from log phase were able to increase the attachment of *G. intestinalis* trophozoites to Caco-2 cells. Moreover, MVs from *G. intestinalis* could be captured by human immature dendritic cells, resulting in increased activation and allostimulation of human dendritic cells. Lipid rafts participate in the MV biogenesis and in the attachment to Caco-2 cells. Nevertheless, proteomic analysis from MVs has shown no significaant differences at the protein levels. An understanding of biogenesis and MV content of MVs derived from trophozoites might have important implications in the pathogenesis of the disease.

Introduction:

Cell-cell communication is mediated by secreted biomolecules, including peptides, proteins, lipids and nucleic acids. These molecules are also present in extracellular vesicles (EVs: mainly exosomes and microvesicles), which are released from different cell types and are able to bind to receptors on target cells, triggering intracellular signalling that modifies the physiological state of the target cells (Ratajczak et al. 2006).

EVs are found at elevated levels in cancer and in different acute and chronic inflammatory diseases including sepsis, stroke, atherosclerosis and diabetes mellitus (reviewed in Loyer X et al, 2014; Aurelian SM et al, 2014). They are also found in physiological processes such as coagulation (Julich et al 2014).

Recently, many authors have described the involvement of EVs during the parasite-host interaction. These authors have shown the presence of EVs of different sizes carrying microRNAs, proteins and pro-inflamatory cytokines modulating the host cell (Marcilla et al. 2014; Evans-Osses et al., 2015; Barteneva et al, 2013)

As the leading cause for protozoal diarrhoea worldwide, the intestinal parasite *Giardia intestinalis* (Syn *G. duodenalis*, *G. lamblia*) is an important pathogen of humans and animals causing morbidity and adversely affecting economies. *Giardia* has a peculiar biology and represents an interesting biological model to understand evolution, organelle function, and antigenic variation (Adam, 2001).

Giardia intestinalis has two evolutionary stages, the trophozoite, which is located in the gut of animals and humans and which multiplies by binary fission, and the infectious stage, the cyst, released into the environment in faeces.

Giardia belongs to the phylum Diplomonadida, unicellular eukaryotes that have undergone considerable reductive evolution. The lateral gene transfer (LGT) mechanism, an important evolutionary step in prokaryotes, has been shown in *Giardia*, supporting this parasite to be included in an early branch of eukaryotic evolution (Embley TM, Hirt RP, 1998). These findings provide insights into the evolution of biochemical pathways in early eukaryote evolution, and could be important in understanding the minimization, or even loss, of most cellular systems such as mitochondria, peroxisomes, Golgi apparatus, and a classical endo-lysosomal system.

Pathological cysts are ingested via the oral route and symptoms usually occur after an incubation period of 1–2 weeks., although half of *Giardia* infections are asymptomatic. After emergence from cysts, the flagellated *G. lamblia* trophozoites colonize mainly the upper small intestine. Trophozoites reside and replicate in the intestinal lumen and at intestinal epithelial cells, but are not able to invade the mucosa. Although still poorly understood, it is clear that the attachment of the parasite to the mucosal surface is the critical point for its persistence in the host. The parasite contains a ventral disk that seems to be important for attachment (Woessner and Dawson, 2012), while the flagella contributes to correct positioning and orientation of the trophozoites before the attachment. The parasite actively engages mucosal immunity and the infection progresses with a low or absent inflammation in most cases (Oberhuber et al., 1997). Most likely, mechanical effects, or some other, as yet not described mechanism, produces villus and brush border microvillus atrophy, leading to digestive enzyme deficiencies (Solaymani- Mohammadiand Singer, 2011), and chronic giardiasis can lead to mucosal inflammation with pronounced villus loss (Hanevik et al., 2007); protease activities may be a direct cause of diarrhoeas in giardiasis. Moreover, Jimenez et al. (2004) found that excretory and secretory antigens (E/S Ags) from *G. lamblia* induced an intestinal pathogenesis, which coincided with mucosal inflammation in BALB/c mice. Oral administration of the E/S Ags not only stimulated production of antibodies with parasiticidal activity, but also resulted in histological alterations within the intestinal tissue that were comparable to those observed in natural and experimental *Giardia* infections. After colonization the cyst formation represents a key step in the life cycle of the parasite. This process involves cellular and molecular events . Lujan H.D et al, 1996 reported that cholesterol starvation induces encystation.

Three encystation- specific cyst wall proteins (CWP1, 2 and 3) are expressed and concentrated in encystation-specific-vesicles (ESVs) that circulate within the parasite before being transported to the cyst wall (Lujan et al, 1996 ; Reiner DS et al, 1990; Lauwaet T et al, 2007; Benchimol and de souza, 2011). Synthesis of ESVs starts 4-6 hours after encystation is induced and is completed with the cyst formation by approximately 24 hours (Reiner DS et al, 1990).. Interestingly, the protozoan could be able to release other kinds of vesicles

that could be speculated to be associated with the attachment to the intestinal cells and pathogenesis. In preliminary work (Deolindo et al, 2013) we have shown that *G.Intestinalis may release MVs when exposed to fferent pHs and inducers. Now,* We have continued an in depth analysis of MV biogenesis and of the phenotype of the extracellular vesicles released by the parasite.

We have hypothesizedin this work that the response of *Giardia intestinalis* to environmental stress conditions results in the active release of MVs from the plasma membrane that modulate the host-parasite cell interaction.

Materials and Methods

Cell culture

A human colonic adenocarcinoma cell line, Caco-2 cell clone C2BBe1 [30], was obtained from the American Type Culture Collection (CRL-2102). Caco-2 cells (passages 57–72) were cultured at 37°C, 5% CO_2 in Dulbecco's Modified Eagle's medium (DMEM; Cellgro, Manassas, VA) supplemented with 10% foetal bovine serum (FBS) (Life Technologies, Grand Island, NY), 100 U/ml penicillin, and 100 mg/ml streptomycin. Cells were fed every third day and passaged using 0.025% trypsin with 0.22 mM EDTA when 80–90% confluent.

Parasite culture and *in vitro* encystation

Giardia lamblia strain WB clone C6 was obtained from the American Type Culture Collection (#50803). Parasites were grown in filter sterilized modified TYI-S-33 medium with 10% adult bovine serum and 0.05% bovine bile at 37°C in microaerophilic conditions and subcultured when confluent. To collect parasites for experiments, the medium was removed from the culture to eliminate unattached or dead parasites. The tube was refilled with cold, sterile medium and trophozoites detached by chilling on ice for 15 min. Parasites were collected by centrifugation (1500 x *g* for 5 min at 4 ºC) and washed once with the plating medium of 90% complete DMEM / 10% Giardia medium. Parasites were then counted using a hemocytometer, and diluted to the appropriate number.

Encystation was induced as described previously (McCaffery and Gillin 1994). Briefly, the pre-encysting cultures were grown to late log phase for 48 h in TYI-S-33 medium (pH 7.1) without antibiotics. Encystation was initiated by removing the spent medium and non-adherent cells and re-nourishing the adherent cells with an encystation medium

(TYI-S-33 medium adjusted to pH 7.8 and supplemented with 0.25 mg/ml bovine bile and 5 mM lactic acid).

Inhibition of Lipids Rafts . Trophozoites from *G. intestinalis* stationary phase were decanted, washed and ressuspended in TYI-S-33 medium without FBS. The parasites were incubated with 2.5, 5.0 and 10 µM de MβCD for 1 hour at 37 C. After this time the parasites were centrifugated at 1000 x *g* for 10 min and the pellet ressuspended with fresh TYI-S-33 medium and used in microvesiculation and adhesion essays.

Adhesion assay. The assay was carried out with stationary phase cultures of *G. Intestinalis* trophozoites or with *G. intestinalis* trophozoites treated with MβCD (10 µm). The parasites were decanted by chilling for 10 min in ice-cold PBS, at pH 7.2. Trophozoite suspensions were centrifuged at 1000 x *g* for 10 min and resuspended to a concentration of $1x10^6$ / ml . Caco cells were seeded on a coverslip in a concentration of $1x\ 10^5$ cells/ well. Suspensions of trophozoites were then co-incubated with cultured cells in a 10 :1 ratio. Plates were incubated at 37°C in 10 % CO_2. After incubating for 1-3 h, unattached trophozoites were counted in a haemocytometer and the % adhered cells determined . The effect of MVs were tested in the same experiments incubated with different concentrations of purified MVs.

Monocyte isolation

Cells were obtained from leukocyte residues of healthy donors from the Blood and Tissue Bank (Barcelona, Spain). Peripheral blood mononuclear cells (PBMCs) were isolated by density gradient centrifugation using Ficoll-Paque (GE Healthcare, Sweden) and T cells (CD3+) were depleted using the RossetteSep Human CD3 Depletion Cocktail (StemCell Technologies, Seattle, USA). PBMCs depleted of T cells were washed twice with washing buffer (400 x *g*, 5 min, RT) and were counted using PerfectCount Microspheres (Cytognos, Salamanca, Spain).

Monocytes were then obtained by positive magnetic selection using the Easysep Human anti-CD14 Positive Selection Kit (Stemcell Technologies, France) following the manufacturer's instructions. Monocytes were >95% CD14+ and viable (as determined by 7-AAD staining).

Differentiation to iDCS

Monocyte-derived dendritic cells (MDDCs) were generated by culturing monocytes with the differentiation cytokines IL4 and GM-CSF for 6 days. Subsequently, isolated monocytes were cultured at 1 x 10^6 cells/ml in complete medium composed of RPMI 1640 (PAA, Pasching, Austria) supplemented with 5% (v/v) heat-inactivated human serum AB (BioWhittaker, Lonza), 2 mM L-glutamine (Sigma Aldrich, USA), 100 U/ml penicillin (Cepa, Spain) and 100 U/ml streptomycin (Normon Laboratories, Spain), with recombinant human IL-4 and GM-CSF (Miltenyi Biotech), both at a final concentration of 1000 U/ml. After six days, immature dendritic cells (iDCs) were harvested by collecting all media and incubating adhered cells with accutase (PAA, Pasching, Austria) for 30 minutes at 37ºC. iDCs were then washed with PBS (400 x *g*, 5 minutes), counted and used for indicated experiments.

Generation of MVs

Plasma Membrane Vesicles (MVs) were produced from the *Giardia intestinalis* trophozoite. Parasites were grown in TYI-S-33 medium with 10% adult bovine serum and 0.05% bovine bile at 37°C in microaerophilic conditions and subcultured when confluent. To collect parasites for experiments, the medium was removed from the culture to eliminate unattached or dead parasites. The tube was refilled with cold, sterile medium and trophozoites detached by chilling on ice for 15 min. Parasites were collected by centrifugation (1500 x *g* for 5 min at 4 ºC) and were then counted using a hemocytometer, and diluted to 1x10^6 cells/ ml. The parasites were incubated in 1ml serum-free culture medium (Yi-S) and stimulated with 1mM $CaCl_2$ for 1h at 37ºC. This way, MV production was stimulated so it prevailed over exosome release, and thus an enriched MVs-containing medium was obtained. After incubation, all medium was collected, centrifuged at 2,500 x *g* for 5 min and the supernatant was further centrifuged twice at 4,000 x *g* for 30 min. Afterwards, supernatant was ultracentrifuged at 100,000 x *g* for 1h 30 min and the pellets, containing concentrated MVs, were collected. MVs were suspended in PBS and were approximately quantified according to their protein content (Bradford assay). Finally, MVs suspensions were dried using speed vacuuming for storage and shipping. Dried MVs were resuspended in PBS and kept at 4ºC until further use.

Flow cytometry

MVs were quantified by counting in a BD FACScalibur™ Flow Cytometer (Becton, Dickinson and Company) using dot plots with SSC and FSC in log scale. Quantification of MVs by FACS analysis was further validated by protein quantification with the Bradford assay.

For surface phosphatidylserine detection MVs were ressupendend in 200 µl of annexin-binding buffer (ABB - HEPES 10 mM, NaCl 140 mM, $CaCl_2$ 2.5 mM, pH 7.2) and incubated with 25ug/ml AnnexinV-FITC (Sigma-Aldrich) for 30 min at room temperature. MVs were diluted in 5 ml of ABB and centrifuged at 100.000 x g during 90 min. The MV pellet was resupended in 500 µl of ABB and data were collected in a flow cytometer (FACSCalibur, BD Biosciences).

MV staining

MVs were stained with the lipophilic dye PKH-67 (Sigma Aldrich, USA) for capture assays. 6µl of PKH-67 was diluted in 1 ml of diluent Cand MVs were also diluted 1/40 in diluent C. Both dilutions were mixed together at a volume ratio of 1:1, and labelling was continued for 15 min at room temperature in the dark. The reaction was stopped by adding 2 ml EV-free FBS (>16h at 100,000 x *g*), and MVs were then washed in PBS, and ultracentrifuged at 100,000 x *g* for 1h 10min (SW28 rotor, OptimaTM XL-100K Ultracentrifuge, Beckman).

NanoSight analysis

EVs were resuspended in 100 µL of PBS, 50 µL of which was diluted 1:10 with 450µL of PBS, and analyzed using NanoSight LM10 equipment and NTA software version 2.3 (NanoSight Ltd, Malvern, UK). Images were recorded for 60s (5 technical replicates) with the folllowing parameters: camera shutter - 1492, camera gain - 512, detection threshold - 10.

MVs capture assay

To assess the ability of iDCs to capture MVs, 10^5 iDCs were incubated at 37ºC in 5% CO_2 with PKH-67 labelled MVs (25 µg or 12.5 µg) at a final volume of 150 µl complete

medium. As a control, iDCs were incubated at 4ºC. Several incubation times were assessed in the different experiments.

After incubation, cells were extensively washed in cold PBS. At this point, they were either stained for capture and phenotype analysis by flow cytometry or left in complete medium at 37º C for a further 24 hours. After culture, cells were assessed for expression of both activation markers and for allostimulation capabilities. For phenotype analysis, the following murine mAbs were used (BD Biosciences): CD83-APC, HLA-DR-APC-H7, CD25-PE and CD25-PE-Cy5. Isotype-matched mAbs were used as controls. All analysis was performed in a FACS Canto II flow cytometer (BD Biosciences) and analysed using FlowJo software. For inhibition experiments, cells were treated for 30 min at 37ºC with cytochalasin D (Calbiochem, Germany) at the indicated concentrations prior to the addition of MVs.

Allostimulation assay

Allostimulation assays were performed by culturing together 1h-MV pulsed, 24h-resting MDDCs with allogeneic CFSE-labelled T cells. T cells were isolated from healthy donors' PBMCs by negative magnetic selection using the Easysep Human T cell Enrichment Kit (Stemcell Technologies), and stained with CFSE (0.4 µM; Invitrogen).

iDCs were co-cultured with T cells at different ratios, from 1:20 (5,000 MDDCs: 100,000 T cells) to 1:160 (625 MDDCs: 100,000 T cells). As a positive control, T cells were stimulated with Phorbol 12-Myristate 13-Acetate (PMA, 0.6 ng/ml, Sigma Aldrich) and Ionomycin calcium salt (200 ng/ml, Sigma Aldrich).

After 4.5 days of culture, proliferation was assessed by flow cytometry (LSR Fortessa Analyzer, BD). Proliferative T cells were gated by diluted CFSE intensity.

Cytotoxicity (viability) tests

We used 5,000 Da (Wako Pure Chemical Industries Ltd., Osaka, Japan) or 500,000 Da (Nacalai Tesque Inc., Kyoto, Japan).??????? Cell viability assays were performed according to our previously reported method. Cells were inoculated in 96-multiwell plates (Costar, Corning, NY, USA) at a cell density of 1.2×10^5 cells/well. At confluence, cells were incubated with serially diluted DSS for pre-determined time periods. DSS was dissolved in culture media and filter-sterilized using a 0.45 µm filter.

Viability was assayed by a commercially available kit (Cell Titer 96™ AQueous, Promega, Madison, USA), which depends on the physiologic reduction of MTS to formazan. Analyses were performed in triplicate.

Confocal microscopy assays.

To corroborate MV capture and examine the distribution of MVs in pulsed iDCs, 10^5 iDCs were incubated with PKH-67-labelled MVs from *Giardia intestinalis* at 37ºC for the indicated periods. Then, cells were extensively washed, stained for CD11c-PE (ImmunoTools), and fixed with 2% formaldehyde solution. Fixed cells were mounted in Immunofluorescence slides with ProLong® Gold Antifade Reagent with DAPI (Life Technologies), and were examined in an Axio-Observer Z1 inverted fluorescent Microscope (ZEISS, Germany).

To determine the endocytosis trafficking, MVs-pulsed iDCs were stained for the Early Endosome Antigen (EEA-1; BD Transduction Laboratories) and Transferrin Receptor (TfR; Abcam, UK), followed by Alexa546-anti mouse IgG and anti rabbit IgG, respectively. Labelling was performed with the IntraStain fixative and permeabilization kit (Dako, Denmark). Finally, cells were cytospun onto glass slides and mounted with ProLong® Gold Antifade Reagent with DAPI. Confocal microscopy was performed on an Axio-Observer Z1 microscope with the LSM 70 confocal module (ZEISS, Germany).

Proteomic assays.

Samples were digested with sequencing grade trypsin (2.5 ng/µL; Promega) as described elsewhere (Shevchenko, A et al, 1996). The digestion mixture was dried in a vacuum centrifuge, resuspended in 50 µL of 2%ACN, 0.1% TFA 1 µl of each digested mixture were loaded onto a trap column (NanoLC Column, 3µ C18- CL, 100umx15cm ;Nikkyo), and desalted with 0.1% TFA at 2µl/min during 10 min. The peptides were loaded onto an analytical column (LC Column, 3 µ C18- CL, 75umx12cm, Nikkyo) equilibrated in 5% acetonitrile 0.1% FA (formic acid). Peptide elution was carried out with a linear gradient of 5 to 35% buffer B in 120 min (A: 0.1% FA; B: ACN, 0.1% FA) at a flow rate of 300nl/min. Peptides were analyzed in a mass spectrometer nanoESI qQTOF (5600 TripleTOF, ABSCIEX). The tripleTOF was operated in information- dependent acquisition mode, in which a 0.25- s TOF-MS scan from 350–

1250 m/z, was performed, followed by 0.05- s product ion scans from 100–1500 m/z on the 50 most intense 2- 5 charged ions. The MS/MS information (combined from three runs of one sample) was sent to MASCOT v2.3.02 or to PARAGON via the Protein Pilotv 4.5 (ABSciex).

MASCOT search engine (Matrix- Science). Database search was performed on NCBInr *Giardia* EST. Searches were performed with tryptic specificity allowing one missed cleavage and a tolerance on the mass measurement of 50 ppm in MS mode and 0.6 Da for MS/MS ions. Carbamidomethylation of Cys was used as a fixed modification and oxidation of Met, and deamidation of Asn and Gln as variable modifications.

ProteinPilot v4.5. search engine (ABSciex). ProteinPilot default parameters were used to generate peak list directly from 5600 TripleTof .wiff files. The Paragon algorithm of ProteinPilot was used to search the NCBI protein database with the following parameters: trypsin specificity, cys- alkylation, no taxonomy restriction, and the search effort set to through. To avoid using the same spectral evidence in more than one protein, the identified proteins were grouped based on MS/MS spectra by the Protein- Pilot Progroup algorithm. Thus, proteins sharing MS/MS spectra are grouped, regardless of the peptide sequence assigned. The protein within each group that can explain more spectral data with confidence is shown as the primary protein of the group. Only the proteins of the group for which there is individual evidence (unique peptides with enough confidence) are also listed, usually toward the end of the protein list.

Results

1-**Trophozoites from *Giardia intestinalis* release extracellular vesicles (MVs) from the plasma membrane under different environmental conditions.**

To simulate the dramatic environmental changes during the cell cycle of *Giardia intestinalis,* we compared the growth curve of trophozoites cultured *in vitro* for 48 h under different pHs ranging from 5 to 8. A poor growth was obtained at pH 8.0, and the best condition was at pH 7.0. Curiously, the parasite was able to grow at acidic pHs (pH 5.0 and 6.0), and the growth was highly inhibited at pH 8.0., a condition in which trophozoites are differentiated to cyst when the parasites are in the presence of inducers such as bile, (Figure 1A). Due to these growth curve differences, we next analysed whether the trophozoites could release MVs in response to different environmental conditions (Figure 1B). We saw a high release of MVs at 24 h at pH 7.0, and no differences were found at different pHs after 48 h (Figure 1C).

We also analyzed the production of MVs during the first 3 h in a serum-free medium with added calcium, a well-known microvesicle inducer, and we detected an increase of MV release between 30 to 120 min, maintaining the release up to 180 min (Figure 1D). On this basis, we decided to perform an experiment of MV induction for 60 min only.

To characterize the type of MVs released by the trophozoite forms of *Giardia intestinalis*, we analyzed the supernatant of trophozoites cultured in a fetal bovine serum-free medium for 60 min in the presence of 1 mM of calcium, and subjected to different rounds of centrifugation and final ultracentrifugation. Examination of the preparation by electron microscopy revealed cup-shaped vesicles of 60–150 nm (Not shown) . MVs were also quantified by FACS and analyzed for size and granularity and the presence of phosphatidylserine by detecting annexin V-FITC staining (Supplementary Fig. 1). We verified the impact of calcium on MV release using higher concentrations of calcium, as well as EGTA (calcium chelating inhibitor), and a calcium ionophore, an activator of calcium release, as shown in the figure 1E.

To determine vesicle size variation in the population of extracellular vescicles, we used nanoparticle tracking analysis (Nanosight, Costa Mesa, CA) to directly examine millions of vesicles. This analysis showed a peak with a mean diameter of 166 nm and that 80 % were between 130 –150 nm in diameter (Fig. 1F and 1 G)

2- **The origin of microvesicles is plasma membrane and lipid raft dependent.**

Due to the size of MVs and presence of phosphatidylserine at the surface, we were interested to verify plasma membrane and lipid raft (also named DRMs (detergent-resistant membranes)) involvement in the biogenesis of *G. intestinalis* MVs. We investigated whether the disruption of lipid rafts from trophozoite plasma membranes affected MV formation, as it was defined previously (Ian del Conde et al, 2005). To assess this effect, we treated trophozoite forms with MβCD **(**methyl-β-cyclodextrin**)** at different concentrations, and we saw a dose-dependent inhibition of MV formation from 25 to 60 % with increasing MβCD (2.5 µM to 10 µM), showing that the depletion of membrane cholesterol decreases EMV formation (Figure 2 A).

The inhibition of MV formation by removal of cholesterol suggests that trophozoites of *G intestinalis* may diminish the parasite's ability to attach to host cell.????????WHY We next performed the adhesion assay using trophozoites either non-treated or treated with 2.5- 10 µM of MβCD, and we detected a dose-dependent inhibition of the attachment of *G. intestinalis* to host cells (Figure 2B).

The importance of lipid raft structure and MV release in the attachment to the host cell was notably verified when *G intestinalis* treated with 5 µM of MβCD was used in an adhesion assay for 3 h in the presence of MVs. We saw that the parsites treated with 5 µM MβCD were unable to attach to Caco-2 cells, and the addition of MVs restored the ability to attach in a dose-dependent manner (Figure 2C) ?????where is this??. These results suggest that MVs bring back certain physical properties to the membrane of the trophozoites, and probably increase the presence of a putative molecule-receptor ligation.

3- **Trophozoites from *Giardia intestinalis* secrete MVs that aid parasite attachment to host cells.**

To investigate whether MVs from *G. intestinalis* could facilitate the adhesion of trophozoites to host cells, we performed an adhesion assay using monolayers of Caco-2 cells, that resemble the enterocytes lining the small intestine, and trophozoites of *G intestinalis* WB strain. Monolayers of Caco-2 cells in the semi-confluent state were incubated with $1x10^6$ trophozoites of *G. intestinalis* in the presence of different concentrations of MVs from *G. intestinalis*, for 1 and 3 h at 37 ºC and 5 % CO_2. Cells were then washed, stained with Giemsa and quantified by light microscopy. We detected a slight dose-dependent increase of *G intestinalis* attachment to Caco-2 cells at

1 h, and a strong 3-fold increase of adhesion of *Gintestinalis* to intestinal cells when parasites and host cells were incubated with 7 µg of MVs compared to that without MVs. (Figure 3 A). Microvesicles treated with proteinase K ((0.05 mg/ml; SigmaAldrich)for 1 hour at 37°C and heat inactivated for incubation at 95°C for 10 minutes were used as adhesion assays controls. The treated-MVs had no effect on the attachment of trophozoites to Caco cells (not shown)

To analyze the specificity of this MV-mediated effect, we next used MVs of *Gintestinalis* in an invasion assay, using metacyclic trypomastigotes forms of *T. cruzi* and Vero cells. Even using higher concentration of MVs (10 µg), the rate of metacyclic trypomastigotes invasion was not modified in the presence of *G intestinalis* MVs that the Mvs could have a specific effect on the parasite and not on Vero Cells.(data not shown). **Too much data not shown???**

4- **MVs communicate with neighbouring cells and face innate immunity**.

Having shown the importance of MVs for cell adhesion, we next investigated the impact of MVs on neighbouring cells and in stimulating innate immunity. For this purpose, we analysed the effect of MVs on the viability of Caco-2 cells and the ability of MVs to be captured by and modulate DC function.

Firstly, Caco-2 cells were incubated in the presence of different concentrations of MVs derived from *Gintestinalis* for 24 and 48 h, and a MTS viability assay was performed. After three independent experiments, we did not detect any effect on the viability of Caco-2 cells using different concentrations of MVs (Figure 3B). We then analysed the interaction between MVs and DCs. Vesicles from GI were labelled with the aliphatic fluorophore PKH-67, and the interaction between MVs and iDCs was assessed by capture, phenotype of capturing cells, and alloproliferation analysis (Figure 4).

Time-course experiments revealed that *G. intestinalis* MVs are rapidly internalized by iDCs (30-40% positively labelled cells only 30 minutes after pulse). Of note, capture of MVs did not affect viability of iDCs (Figure 4A, 4B). Noticeably, capture was inhibited almost completely at low temperature (4ºC) and by the addition of cytochalasin D to the iDC culture, thus indicating a clear endocytic component on the capture of MVs (Figure 4BandC). MV internalization was confirmed also by inverted fluorescent microscopy, and cells pulsed at 4ºC showed no MVs within them (Figure 4D). To further confirm the involvement of the endocytic pathway in the MV capture by iDCs, confocal images were taken at short time intervals. Five minutes after incubation, captured MVs

colocalized with the early endocytosis marker Transferrin Receptor (TfR) (Figure 4E). At later time points (15 min of incubation), MVs colocalized with the Early Endosome Associated protein (EEA-1, Figure 4E), and after one hour of incubation, cells showed sac-like compartments where captured MVs probably aggregated all together (Figure 4D).

To assess the capacity of MVs to induce DC maturation, iDCs were pulsed for one hour with MVs, washed, and further cultured for 24 h. At this time point, classical activation markers such as CD83 and HLA-DR did not vary their expression. However, GI-MVs-capturing iDCs upregulated the activation marker CD25 (Figure 5A) suggesting a mild activation of iDCs. This mild activation was further confirmed by the increase of alloantigenic stimulation potential of DCs in T cell alloproliferation experiments (Figure 5B).

5- **Proteomic and RNA analysis of MVs suggest a modulation effect to host cells.**

We investigated the content of MVs released by mid-log trophozoites and by trophozoites induced to Cyst form by proteomic assays. The mass spectrometry analysis showed differences in the content of these MVs (Table 1). Only 11 proteins were identified from the trophozoite stage, seven of them previously reported as present in MVs in other organisms as described in the vesiclepedia (Kalra et al., 2012; http://microvesicles.org). In the case of MVs from cyst transition, 80 proteins were detected (36 of them still unknown), and from the 44 remaining, 24 proteins corresponded to previously identified EVs proteins (Table 1). Interestingly, in the cyst stage, proteins involved in pathogenesis like VSPs and giardins were identified in MVs (Table 1). Further investigation is needed to identify specific markers released by the different MV populations.

When analysing the RNA content of MVs released by trophozoites, there was a presence of miRNA produced by calcium induction in trophozoites forms (Figure S1). Interestingly, when we compared the total RNA from non-induced trophozoites with trophozoites activated to produce MVs, a clear difference was noticed, where the miRNA in trophozoites producing MVs contained the miRNAs that appear in MVs purified after induction. (Fig S1).

Discussion

1- **Trophozoites from *Giardia intestinalis* respond to environmental changes releasing MVs that facilitate the interaction with host cells.**

The results presented in this study have demonstrated that trophozoites from *Giardia intestinalis* are able to release MVs in response to different pH levels, and calcium (Figure 1). Many reports have shown the secretion of MVs during an interaction of protozoans with host cells. One interesting example of the role of MVs affecting the environment is the murine malaria model infected with *Plasmodium berghei*, which develops cerebral malaria (CM). EVs isolated from plasma derived from infected erythrocytes resulted in a potent activation of macrophages via toll-like receptors, whereas plasma-derived MVs from naïve animals did not induce macrophages (Couper et al., 2010). In the same murine model, the abrogation of MVs formation in mice knocked out for the gene *ABCA1* protected these animals against CM, demonstrating a link between EV production and pathogenesis (Combes et al., 2005).

In *Trypanosoma cruzi*, Cestari et al. (2012), demonstrated that metacyclic trypomastigotes forms when in contact with the monocytic THP-1 cell line, release MVs that inhibit C3 convertase, and aid the parasite to invade host cells. Recently, other groups have shown that MVs from *T. cruzi* have different sizes, and different effects. Bayer-Santos et al. (2013), found two types of EVs secreted by the parasites. Later, Garcia-Silva et al. (2014); Linhares-Lacerda et al. (2015), and Fernandez-Calero et al. (2015) showed the involvement of miRNA in MV transfer to host cells, indicating this mechanism as a novel modulating effect against neighbouring cells.

Other reports have also described that the protozoan *Trichomonas vaginalis* secretes extracellular vesicles similar to mammalian exosomes. The parasite-derived exosomes contain RNA, conserved exosomal proteins and parasite-specific proteins (Twu et al., 2013). They also demonstrated that *T. vaginalis* exosomes are able to deliver their contents to host cells and modulate host cell immune responses. Interestingly, exosomes from highly adherent parasite strains increased the adherence of poorly adherent parasites to vaginal and prostate epithelial cells. In contrast, exosomes from poorly adherent strains had no measurable effect on parasite adherence (Twu et al., 2013). We

believe that *Giardia intestinalis* release MVs as a response to differences in the environment, and this is a likely consequence of limited organelle specialization in this protozoan (Faso and Hell, 2011).

2- **Microvesicle release is associated with lipid rafts and MVs are derived from the plasma membrane**.

The mechanism of MV release has been associated with induction or stimulation of cells producing an increase in intracellular calcium, which is mobilized by calpain in turn inhibiting flippase and activating scramblease. The biophysical step including the exovagination of the phospholipid bilayer is a mechanism still poorly understood. Different reports have shown that cholesterol should influence the lipid raft microdomains on the membrane that participate in MV formation. An interesting report by del Conde et al. (2005), demonstrated that the coagulation process is dependent of the transference of tissue factors released from monocyte-MVs to platelets. This release is dependent of lipids raft microdomains. Moreover, the shedding of MVs containing tissue-factor was abolished with the depletion of membrane cholesterol. Interestingly the giardia genome (Giardia DB) has no annotation to GPI-anchor proteins, a family of proteins associated to sphingolipids and cholesterol on the plasma membrane and related to lipid raft formation. However a putative transamidase annotated could be transferring GPI to other acceptors. The recently described genome in *G. intestinalis* (Morrison et al, 2007) revealed the presence of lipids synthesis and metabolic genes. Which proteins and structures are related to lipids rafts formation need to be validated. Recently De Chaterjee et al. (2015) hypothesized that Lipids rafts act as molecular sensors on the plasma membrane. They used conjugated cholera toxin B (CTXB) which binds GMI glycolipid demonstrating lipid rafts at the membrane, ventral disc and caudal flagella. Moreover nystatin and filipin III, two well known LR disrupting agents inhibited the CTXB binding indicating that lipid rafts contain cholesterol and the removal destabilized the microdomains. De Chaterjee et al. (2015) discussed the possible connection between lipids rafts and sphingolipids metabolism in Giardia regulating the encystation process.

Our findings support the involvement of cholesterol in MV release, as we observed an inhibition of MV production using different concentrations of MβCD (Figure 2A). Furthermore, the absence of cholesterol inhibited the parasites attachment to the host cell, and it was subsequently restored by the exogenous presence of MVs (Figure 2B).

3-**Microvesicles from *Giardia intestinalis* modulate dendritic cells implicating them in the pathogenesis**

Factors associated with the pathology of giardiasis indicate a likely mechanical alteration of intestinal mucosa for the attachment of the trophozoites, due to the involvement of cystein protease activities secreted by the parasite in contact with host cells. In fact, a lower activation or damage to host cell should be associated with a low inflammation that progresses in giardiasis. Previous work using mouse models to determine the role of various cytokines in immunity to *Giardia* have shown that IL-6 plays a critical role in the control of primary infections with this parasite (Bienz et al., 2003; Zhou et al., 2003). Here, we have analysed whether MVs release by trophozoites should alter dendritic cells, which are a family of professional antigen-presenting cells (APCs), that reside in all peripheral tissues in an immature state, capable of antigen uptake and processing. Dendritic cells (DC) when activated are key to enhanced cytokine secretion and enable DC migration and recruitment of other cell types. DC capture of *Giardia* MVs suggests an effective contact with host cells. Furthermore, *in vitro* or *in vivo* assays could indicate the role of MVs in dendritic cell modulation. Recently, some manuscripts have shown and reviewed the role of dendritic cells during protozoan -host cell interaction (i.e. Weidner et al., 2016; Feijo et al., 2016; Ersshing et al., 2016). However, there are no current reports involving MVs from parasites in modulating dendritic cell functions.

4-**Exosome and microvesicles content can alter neighbouring cells**.

There are numerous examples in the literature of protozoa releasing large amounts of material into the extracellular space as a form of cellular communication with host cells (Garcia-Silva et al., 2014; Linhares-Lacerda et al., 2015; Fernandez-Calero et al., 2015; Cestari et al., 2012). In *Giardia intestinalis*, the diarrhoea and malabsorption could be a direct result of the interaction of the parasite with the intestinal epithelium which might

be mediated by the parasite itself, or by substances it secretes or by MVs that could alter neighbouring cells. Analysis of Caco-2 human intestinal epithelial cells demonstrated that *Giardia* infection resulted in a strong alteration of the expression profile of these cells, including stress-response genes and chemokines, as seen by microarray analyses (Roxstrom-Lindquist et al., 2005). Transcriptional changes in *G. intestinalis* during interaction with intestinal epithelial cells were also monitored by microarray analysis of *G. intestinalis* cDNAs, and indicated up-regulation of genes encoding enolase, cysteine proteinase, arginine deiminase and oxygen defence proteins (Ringqvist et al., 2011). Interestingly, contact of *G. intestinalis* with epithelial cells resulted in the release of metabolic enzymes (arginine deaminase, ornithine carbamoyltransferase and enolase) from *G. intestinalis*, which disabled host immune factors including nitric oxide (Ringqvist et al., 2008). A previous study also demonstrated that the excretory-secretory products (ESP) of *G. lamblia* contained major antigen(s) responsible for protection against infection in mice (Kaur H et al, 1999). Oral administration of *G. lamblia* ESPs into BALB⁄ c mice stimulated a Th2 response, which led to intestinal histological changes characterized by eosinophilic infiltration, and can induce host cell apoptosis, hypercellularity, and enterocytic desquamation (Jimenez et al., 2004). Glycoproteins in *G. lamblia* ESP were found to induce antibody production during giardiasis (Khar et al., 2001; Jimenez et al., 2007). Cysteine proteases present in *G. lamblia* ESP were essential for the induction of antibody and cytokine production in BALB⁄ c mice infected with ESP (Jimenez et al., 2009). Our findings of small RNAs in the cargo of EMVs suggest that the parasite could transfer material to host cells trough EMVs, modifying the cell phenotype. An interesting previous report supports this possibility; the infection of human ileocecal adenocarcinoma cell line HCT-8 with *Giardia intestinalis* can induce host cell apoptosis. Signs of chromatin condensation and caspase 3 activation was found to occur in monolayers exposed to different *G. intestinalis* assemblages (Kho et al., 2013). Nuclear fragmentation and cell death was suppressed with a caspase 3 inhibitor. The most important point was the demonstration that cellular extracts from *Giardia intestinalis* were able to induce apoptosis without contact with the parasite. This fact supports the idea that EVs should alter the host cell. MicroRNAs have been shown to have a role in cancer, cell re-programming, hypertension regulation and other chronic diseases (reviewed by Tao ZQ et al., 2016; Stepicheva and Song, 2016; Makarova et al., 2016), and could be essential in host-parasite cell interactions.

Taken together, our findings and new concepts reveal another facet to the ever increasingly complex environment of dynamic cellular communication between parasites and hosts. The content of MVs, including protein and nucleic acids, may modify the cell phenotype avoiding innate immunity and producing the infection (Figure 6). The identification of cellular targets and inhibitors of microvesiculation could potentially represents a novel strategy to control the diseases, and are currently under investigation.

Acknowledgements

We would like to thank Dr. F.B. to facilitate Senior researcher stay of M.R at the Germans trias e pujol Institute, Badalona, Spain. We also thank to Luz Valero from S.C.S.I.E. Universidad de Valencia for proteomic analysis and Dr. Wanderson Da Rocha for sharing his laboratory at the Universidad Federal de Parana. Finally, this study has received support from FIOCRUZ, CNPq, and Programa Basico de Parasitologia AUXPE 2041/2011 (CAPES), Brazil. M.R is currently fellow from CNPq-Brazil and I.E.O, Was fellow from CAPES.

FIGURE LEGENDS

FIGURE 1. Stress factors in the gastric environment affect growth of *G. intestinalis* trophozoites and their production of MVs: A) Growth at different pH values. An initial inoculum containing $5x10^4$ parasites/ml was cultured at 37ºC for 24 or 48 h in media at different pH values. Subsequently, parasites were quantified using a Neubauer chamber. Results are representative of two independent experiments. B) MV production with different inducers. Trophozoites were induced to release MVs in different conditions, the supernant then being ultracentrifugued, and MV production quantified by flow cytometry. The chart is representative of measurements made in triplicate, and the results represent the mean ± standard error of three independent experiments. C) Effect of pH on MV production by *G. intestinalis* trophozoites. MVs were induced in the presence of $CaCl_2$ and their release was monitored at 24 and 48h time points. EMVs contained in the supernatant were quantified by flow cytometry. The results are representative of measurements made in triplicate ± standard error of three independent experiments. D) Early kinetics of MV production by trophozoites of *G. intestinalis* at pH 7.0 MVs induction was performed with $CaCl_2$ at pH 7 from 0 to 180 min, and the analysis of the release was performed after different incubation times. MVs contained in the supernatant were quantified by flow cytometry. The chart is representative of measurements made in triplicate, and the results represent the mean ± standard error of three independent experiments. E) MV production from *G. intestinalis* trophozoites upon treatment with 1 mM $CaCl_2$, 3µM Calcium ionophore A23187 and 5 mM EGTA. F) Nanosight trace of purified vesicles. A mean diameter of nm was measured. (G) Table from Nanosight analysis of percentage of purified vesicles in various size ranges.

The bar graph represents the mean ± standard error of three independent experiments.

Figure 2 Effect of lipid raft disruption by cholesterol depletion on MV production.

A) The extraction of membrane cholesterol decreases the production of MVs. Trophozoites were incubated with different concentrations of MβCD for one hour. Later the trophozoites were induced with 1 mM of $CaCl_2$, and the MVs released were quantified by flow cytometry. Measurements were made in triplicate and the results

represent the mean ± standard error of three independent experiments. The Student t test was used for statistical analysis. The asterisks WHERE?? indicate the results that were statistically significant ($p < 0.05$) compared to control. B) Treatment of Giardia intestinalis WB with the lipid raft-destabilizing methyl-β-cyclodextrin (MβCD) inhibits their adhesion to Caco 2 cells. Adhesion of WB pre-treated with 0- 10 µM of MBCD to Caco cells was determined for 3 hrs at 37°C. The trophozoites present in the supernatant were quantified by hemocytometer. C) MVs of *Giardia intestinalis* restore the ability of GI WB pre-treated with 5 µM of MβCD to bind to Caco cells. The Adhesion of WB pre-treated with 5 µM of MβCD to Caco cells was determined in the presence of different concentrations of purified MVs of GI for 3 hrs at 37 C. Results represent the mean ± the standard error from two independent experiments. The Student t test was used for statistical analysis. The asterisks indicate the results that were statistically significant ($p < 0.05$) compared to control.

Figure 3 – Effect of *Giardia intestinalis* microvesicles on parasite adherence to Caco-2 cells.

A) Trophozoites adherence to host cells in the presence of MVs. Trophozoites were incubated for 1 h ?? and 3 h ??, with Caco-2 cells in the presence of different concentrations of MVs (previously obtained from trophozoites). The amount of adhering trophozoites to Caco-2 cells was determined by counting the trophozoites present at the supernant in a Neubauer chamber. The conditions were tested in duplicate. As control Isolated vesicles were incubated with proteinase K (0.05 mg/ml; SigmaAldrich) for 10 minutes at 37 C. The Results represent the mean ± standard error of three independent experiments. The Student t test was used for statistical analysis. The asterisks where indicate the results that were statistically significant ($p < 0.05$) compared to control. B) Effect of *G. intestinalis* MVs on viability of Caco-2 cells, $5x10^3$ cells/well being incubated in the presence of different concentrations of MVs from *G. intestinalis* trophozoites for 24 h. Cell viability was assessed by the MTS assay and the results are presented as percentages relative to untreated cells with MVs (control). Measurements were made in triplicate, the results represent the mean ± standard error of three independent experiments. ANOVA with multiple comparisons

was performed the statistical analysis. The asterisks indicate the results that were statistically significant ($p < 0.05$) respect to the control.

Figure 4. MVs from *Giardia intestinalis* are actively captured by human immature dendritic cells (iDCs). A) and B) MVs labelled with PKH-67 were added to iDCs and capture was assessed after 30minutes or 1h at 37ºC or 4ºC without or with further 24h of resting. The percentage of PKH-67$^+$ iDCs was analysed by flow cytometry. A) Representative plots of the capture analysis performed by flow cytometry. B) Mean values of PKH67+ cells ±SD of three independent experiments. C) Active capture by iDCs was corroborated by blocking with Cytochalasin-D incubation 30min prior to EMV addition. The mean ±SD of the viability (%7AAD$^-$ cells) and capturing cells (%PKH-67$^+$ cells) is expressed as relative to the control. D) Inverted fluorescence imaging of iDCs pulsed with PKH-67- labelled MVs confirmed temperature-dependence of EMV internalization by iDCs (CD11c$^+$, red) (b). After one hour of incubation, iDCs aggregate endocytosed MVs in sac-like compartments (c and d). E) MVs are internalized and sorted to the endocytic compartiments of iDCs. Confocal imaging of iDCs pulsed with PKH-67- labelled MVs show co-localization (yellow) with transferrin receptor (TfR, red; a and b), at already 5 min after pulse. Within 15 min, MVs co-localized with the early endocytosis associated protein (EEA-1, red, c and d), showing aggregation of MVs in endosomal compartments.

Figure 5. MVs from *Giardia intestinalis* induce activation and enhance the allostimulation capabilities of iDCs. MVs were added to iDCs and cultured for 1h. After extensive washing and 24h resting, cells were checked for (A) activation marker expression (CD83, HLA-DR and CD25) and (B) allostimulation capabilities towards T cells. A) Fold change expression of the indicated markers, relative to non-pulsed iDCs. Data is depicted as mean ±SD of three independent experiments. B) CFSE-labeled T cells were co-cultured with 1h-pulsed, 24h-resting iDCs at the indicated ratios. Alloproliferation of T cells was analysed according to the percentage of CFSE^{low} cells. Data is representative of three independent experiments.

Figure 6. *G. intestinalis* MVs increase parasite adherence to intestinal epithelial cells but uptake by iDC cells may through their activation help direct a T cell response. (A) *G. intestinalis* trophozoite EMVs increase the adherence of the parasite to

intestinal epithelial cells. (B) *G. intestinalis* MVs are taken up by iDCs which are then activated and mature (showing upregulation of CD25). T cell alloproliferation experiments then showed an increase of the alloantigenic stimulation potential of DCs.

TABLE 1. Proteomic analysis of microvesicles from *Giardia intestinalis* in trophozoites and cyst stages. Genebank accession number, name of the gene, relative abundance by EmPAI data, and presence in homologues dataset of MVs (microvesicles.org) are shown.

Supplementary Figure 1.
Flow cytometric analysis of the MVs of G.intestinalis. The MVs were quantified by flow cytometry (BD FACScalibur) in size and granularity graphs (FSC x SSC). PS exposure analysis was performed with FITC conjugated Annexin V on a FL-1 fluorescence histogram. (A) FSCxSSC plot of MVs labeled with annexin-V-FITC, the population of MVs with surface PS exposure (green, R2) were obtained from a fluorescence histogram (B), as marking control were used MVs without Annexin-V-FITC; (C) 1 mM CaCl2; (D) 3μM Calcium ionophore A23187; (E) 5mM EGTA;

Bibliography

Adam, R.D. (2001). Biology of Giardia lamblia. Clinical Microbiology Reviews *14*, 447–475.

Aurelian SM, Cheţa DM, Onicescu D. Microvesicles - potential biomarkers for the interrelations atherosclerosis/type 2 diabetes mellitus. Rom J Morphol Embryol. 2014;55(3 Suppl):1035-9.

Barteneva, N.S., Maltsev, N., and Vorobjev, I.A. (2013). Microvesicles and intercellular communication in the context of parasitism. Frontiers in Cellular and Infection Microbiology *3*.

Bayer-Santos, E., Aguilar-Bonavides, C., Rodrigues, S.P., Cordero, E.M., Marques, A.F., Varela-Ramirez, A., Choi, H., Yoshida, N., da Silveira, J.F., and Almeida, I.C. (2013). Proteomic analysis of Trypanosoma cruzi secretome: characterization of two populations of extracellular vesicles and soluble proteins. J. Proteome Res. *12*, 883–897.

Benchimol, MDS.; De Souza, W. The ultrastructure of giardia during growth and differentiation. In: Hugo, D.; Luján, SS., editors. *Giardia*: a model organism. Vienna: Springer; 2011

Bienz, M., Dai, W.J., Welle, M., Gottstein, B., and Müller, N. (2003). Interleukin-6-deficient mice are highly susceptible to Giardia lamblia infection but exhibit normal intestinal immunoglobulin A responses against the parasite. Infect. Immun. *71*, 1569–1573.

Boscardin, S.B., Rosa, D.S., Kamphorst, A.O., and Trumpfheller, C. (2016). Dendritic Cells in Tolerance and Immunity against Pathogens. Journal of Immunology Research *2016*, 1–2.

Cestari, I., Ansa-Addo, E., Deolindo, P., Inal, J.M., and Ramirez, M.I. (2012). Trypanosoma cruzi immune evasion mediated by host cell-derived microvesicles. J. Immunol. *188*, 1942–1952.

Combes, V., Coltel, N., Alibert, M., van Eck, M., Raymond, C., Juhan-Vague, I., Grau, G.E., and Chimini, G. (2005). ABCA1 gene deletion protects against cerebral malaria: potential pathogenic role of microparticles in neuropathology. Am. J. Pathol. *166*, 295–302.

Couper, K.N., Barnes, T., Hafalla, J.C.R., Combes, V., Ryffel, B., Secher, T., Grau, G.E., Riley, E.M., and de Souza, J.B. (2010). Parasite-Derived Plasma Microparticles Contribute Significantly to Malaria Infection-Induced Inflammation through Potent Macrophage Stimulation. PLoS Pathogens *6*, e1000744.

Del Conde, I., Shrimpton, C.N., Thiagarajan, P., and López, J.A. (2005). Tissue-factor-bearing microvesicles arise from lipid rafts and fuse with activated platelets to initiate coagulation. Blood *106*, 1604–1611.

Embley TM1, Hirt RP. Early branching eukaryotes? Curr Opin Genet Dev. 1998 Dec;8(6):624-9.

Evans-Osses, I., Reichembach, L.H., and Ramirez, M.I. (2015). Exosomes or microvesicles? Two kinds of extracellular vesicles with different routes to modify protozoan-host cell interaction. Parasitology Research *114*, 3567–3575.

Faso, C., and Hehl, A.B. (2011). Membrane trafficking and organelle biogenesis in Giardia lamblia: use it or lose it. Int. J. Parasitol. *41*, 471–480.

Fernandez-Calero, T., Garcia-Silva, R., Pena, A., Robello, C., Persson, H., Rovira, C., Naya, H., and Cayota, A. (2015). Profiling of small RNA cargo of extracellular vesicles shed by Trypanosoma cruzi reveals a specific extracellular signature. Mol. Biochem. Parasitol. *199*, 19–28.

Garcia-Silva, M.R., Cabrera-Cabrera, F., das Neves, R.F.C., Souto-Padrón, T., de Souza, W., and Cayota, A. (2014). Gene expression changes induced by Trypanosoma cruzi shed microvesicles in mammalian host cells: relevance of tRNA-derived halves. Biomed Res Int *2014*, 305239.

Hanevik, K., Hausken, T., Morken, M.H., Strand, E.A., Mørch, K., Coll, P., Helgeland, L., and Langeland, N. (2007). Persisting symptoms and duodenal inflammation related to Giardia duodenalis infection. Journal of Infection *55*, 524–530.

House, S.A., Richter, D.J., Pham, J.K., and Dawson, S.C. (2011). Giardia Flagellar Motility Is Not Directly Required to Maintain Attachment to Surfaces. PLoS Pathogens *7*, e1002167.

Jiménez, J.C., Fontaine, J., Grzych, J.-M., Dei-Cas, E., and Capron, M. (2004). Systemic and mucosal responses to oral administration of excretory and secretory antigens from Giardia intestinalis. Clin. Diagn. Lab. Immunol. *11*, 152–160.

Jiménez, J.C., Morelle, W., Michalsky, J.-C., and Dei-Cas, E. (2007). Excreted/secreted glycoproteins of G. intestinalis play an essential role in the antibody response. Parasitol. Res. *100*, 715–720.

Jiménez, J.C., Fontaine, J., Creusy, C., Fleurisse, L., Grzych, J.-M., Capron, M., and Dei-Cas, E. (2014). Antibody and cytokine responses to Giardia excretory/secretory proteins in Giardia intestinalis-infected BALB/c mice. Parasitol. Res. *113*, 2709–2718.

Julich, H., Willms, A., Lukacs-Kornek, V., and Kornek, M. (2014). Extracellular Vesicle Profiling and Their Use as Potential Disease Specific Biomarker. Frontiers in Immunology *5*.

Kaur, H., Samra, H., Ghosh, S., Vinayak, V.K., and Ganguly, N.K. (1999). Immune effector responses to an excretory-secretory product of Giardia lamblia. FEMS Immunol. Med. Microbiol. *23*, 93–105.

Kaur, H., Ghosh, S., Samra, H., Vinayak, V.K., and Ganguly, N.K. (2001). Identification and characterization of an excretory-secretory product from Giardia lamblia. Parasitology *123*, 347–356.

Koh WH1, Geurden T, Paget T O'Handley R, Steuart RF, Thompson RC, Buret AG. Giardia duodenalis assemblage-specific induction of apoptosis and tight junction disruption in human intestinal epithelial cells: effects of mixed infections. J Parasitol 2013 Apr;99(2):353-8. doi: 10.1645/GE-3021.1. Epub 2012 Aug 27.

Lauwaet T, Davids BJ, Torres-Escobar A, Birkeland SR, Cipriano MJ, Preheim SP, et al. Protein phosphatase 2A plays a crucial role in *Giardia lamblia* differentiation. Mol Biochem Parasitol. 2007; 152(1):80–89. [PubMed: 17204341]

Linhares-Lacerda, L., Palu, C.C., Ribeiro-Alves, M., Paredes, B.D., Morrot, A., Garcia-Silva, M.R., Cayota, A., and Savino, W. (2015). Differential Expression of microRNAs in Thymic Epithelial Cells from Trypanosoma cruzi Acutely Infected Mice: Putative Role in Thymic Atrophy. Frontiers in Immunology *6*.

Loyer X1, Vion AC, Tedgui A, Boulanger CM. Microvesicles as cell-cell messengers in cardiovascular diseases. Circ Res. 2014 Jan 17;114(2):345-53. doi: 10.1161/CIRCRESAHA.113.300858.

Luján HD[1], Mowatt MR, Byrd LG, Nash TE.
Cholesterol starvation induces differentiation of the intestinal parasite Giardia lamblia Proc Natl Acad Sci U S A. 1996 Jul 23;93(15):7628-33.

Marcilla, A., Martin-Jaular, L., Trelis, M., de Menezes-Neto, A., Osuna, A., Bernal, D., Fernandez-Becerra, C., Almeida, I.C., and del Portillo, H.A. (2014). Extracellular vesicles in parasitic diseases. Journal of Extracellular Vesicles *3*.

McCaffery, J.M., and Gillin, F.D. (1994). Giardia lamblia: ultrastructural basis of protein transport during growth and encystation. Exp. Parasitol. *79*, 220–235.

Oberhuber, G., and Stolte, M. (1997). Symptoms in Patients with Giardiasis Undergoing Upper Gastrointestinal Endoscopy. Endoscopy *29*, 716–720.

Genomic minimalism in the early diverging intestinal parasite *Giardia lamblia*.

Morrison HG, McArthur AG, Gillin FD, Aley SB, Adam RD, Olsen GJ, Best AA, Cande WZ, Chen F, Cipriano MJ, Davids BJ, Dawson SC, Elmendorf HG, Hehl AB, Holder ME, Huse SM, Kim UU, Lasek-Nesselquist E, Manning G, Nigam A, Nixon JE, Palm D, Passamaneck NE, Prabhu A, Reich CI, Reiner DS, Samuelson J, Svard SG, Sogin ML. Science. 2007 Sep 28;317(5846):1921-6.

Reiner DS, McCaffery M, Gillin FD. Sorting of cyst wall proteins to a regulated secretory pathway during differentiation of the primitive eukaryote *Giardia lamblia*. Eur J Cell Biol. 1990; 53(1):142–153.

Ringqvist, E., Palm, J.E.D., Skarin, H., Hehl, A.B., Weiland, M., Davids, B.J., Reiner, D.S., Griffiths, W.J., Eckmann, L., Gillin, F.D., et al. (2008). Release of metabolic enzymes by Giardia in response to interaction with intestinal epithelial cells. Mol. Biochem. Parasitol. *159*, 85–91.

Ringqvist, E., Avesson, L., Söderbom, F., and Svärd, S.G. (2011). Transcriptional changes in Giardia during host-parasite interactions. Int. J. Parasitol. *41*, 277–285.

Roxström-Lindquist, K., Ringqvist, E., Palm, D., and Svärd, S. (2005). Giardia lamblia-induced changes in gene expression in differentiated Caco-2 human intestinal epithelial cells. Infect. Immun. *73*, 8204–8208.

Shevchenko, A., Jensen, O.N., Podtelejnikov, A.V., Sagliocco, F., Wilm, M., Vorm, O., Mortensen, P., Shevchenko, A., Boucherie, H., and Mann, M. (1996). Linking genome and proteome by mass spectrometry: large-scale identification of yeast proteins from two dimensional gels. Proc. Natl. Acad. Sci. U.S.A. *93*, 14440–14445.

Solaymani-Mohammadi, S., and Singer, S.M. (2011). Host Immunity and Pathogen Strain Contribute to Intestinal Disaccharidase Impairment following Gut Infection. The Journal of Immunology *187*, 3769–3775.

Twu, O., de Miguel, N., Lustig, G., Stevens, G.C., Vashisht, A.A., Wohlschlegel, J.A., and Johnson, P.J. (2013). Trichomonas vaginalis exosomes deliver cargo to host cells and mediate host∶parasite interactions. PLoS Pathog. *9*, e1003482.

Woessner, D.J., and Dawson, S.C. (2012). The Giardia Median Body Protein Is a Ventral Disc Protein That Is Critical for Maintaining a Domed Disc Conformation during Attachment. Eukaryotic Cell *11*, 292–301.

Zhou, P., Li, E., Zhu, N., Robertson, J., Nash, T., and Singer, S.M. (2003). Role of interleukin-6 in the control of acute and chronic Giardia lamblia infections in mice. Infect. Immun. *71*, 1566–156

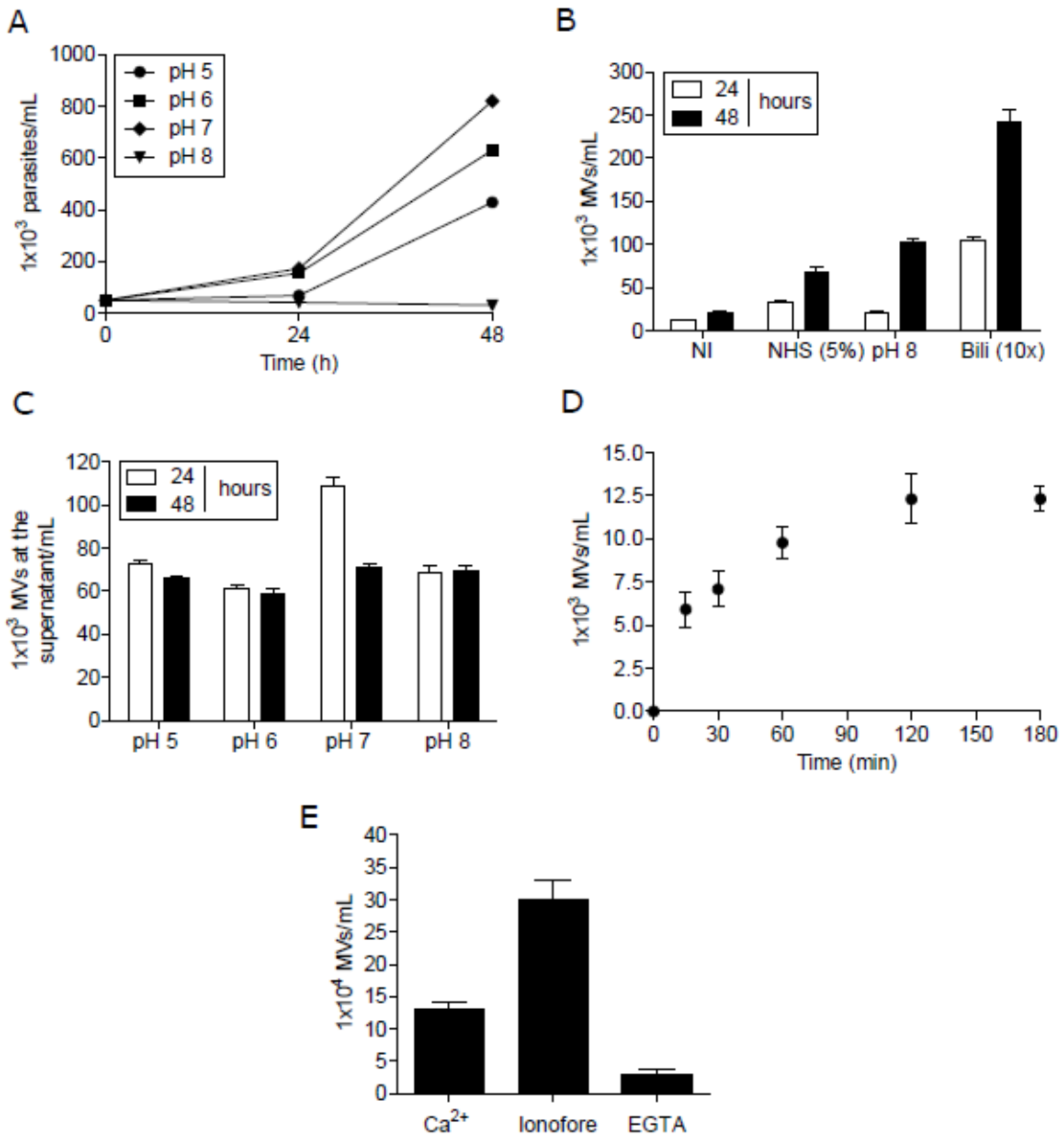
A
1000
800
600
400
200
0
1x10³ parasites/mL
pH 5
pH 6
pH 7
pH 8
0
24
48
Time (h)
B
300
250
200
150
100
50
0
1x10³ MVs/mL
24
48
hours
NI
NHS (5%) pH 8
Bili (10x)
C
120
100
80
60
40
20
0
1x10³ MVs at the supernatant/mL
24
48
hours
pH 5
pH 6
pH 7
pH 8
D
15.0
12.5
10.0
7.5
5.0
2.5
0.0
1x10³ MVs/mL
0
30
60
90
120
150
180
Time (min)
E
40
35
30
25
20
15
10
5
0
1x10⁴ MVs/mL
Ca2+
Ionofore
EGTA

Fig. 1

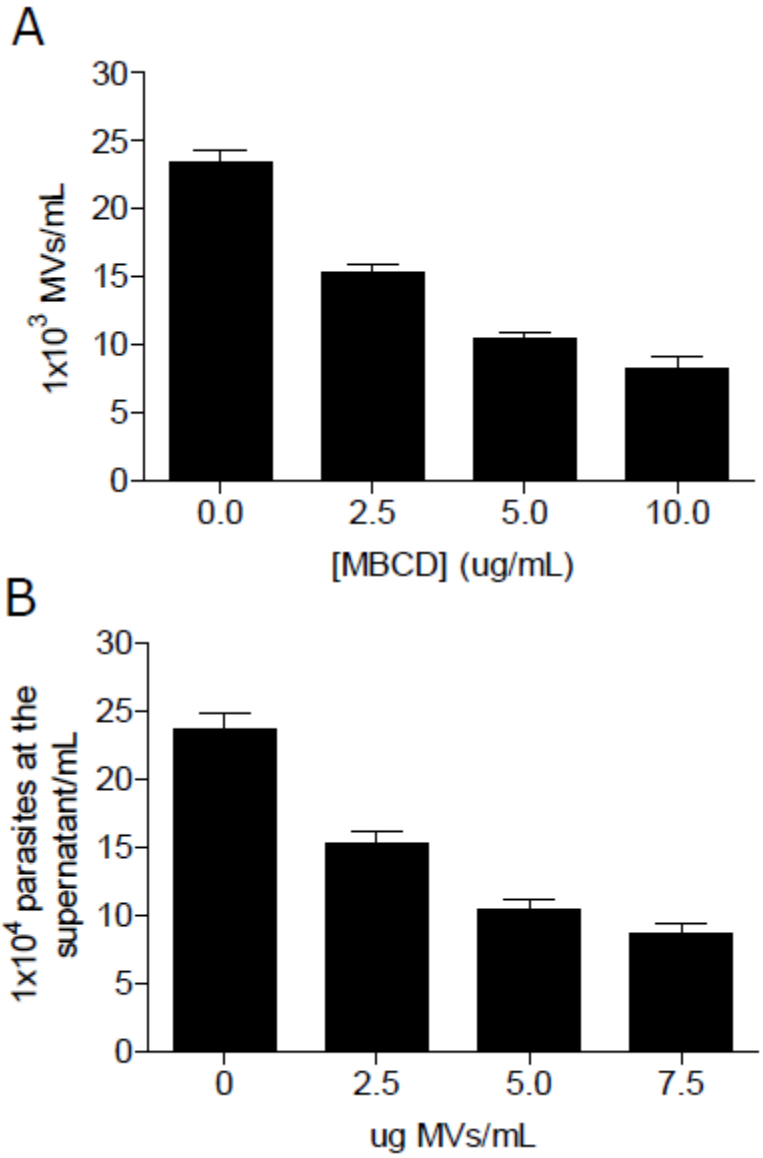
A
30
25
20
15
10
5
0
1x10^3 MVs/mL
0.0
2.5
5.0
10.0
[MBCD] (ug/mL)
B
30
25
20
15
10
5
0
1x10^4 parasites at the supernatant/mL
0
2.5
5.0
7.5
ug MVs/mL

Fig. 2

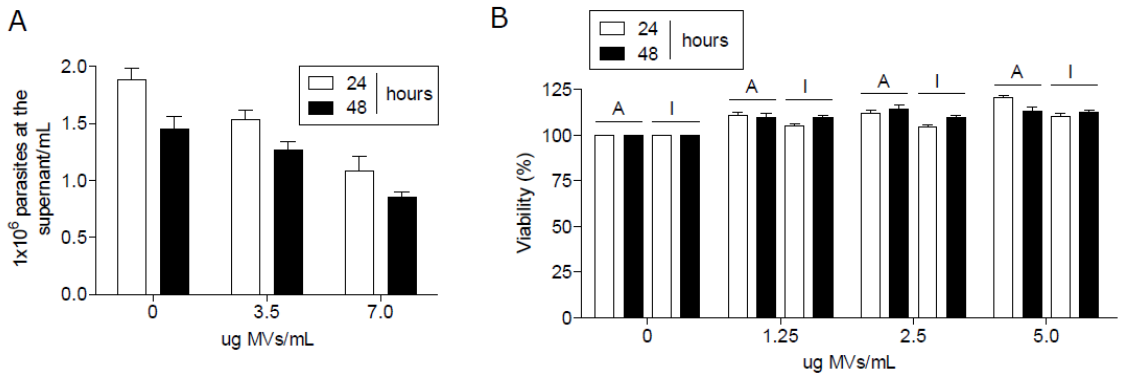
A
1x10^6 parasites at the supernant/mL
2.0
1.5
1.0
0.5
0.0
24
48
hours
0
3.5
7.0
ug MVs/mL
B
24
48
hours
Viability (%)
125
100
75
50
25
0
A
I
A
I
A
I
A
I
0
1.25
2.5
5.0
ug MVs/mL

Fig. 3

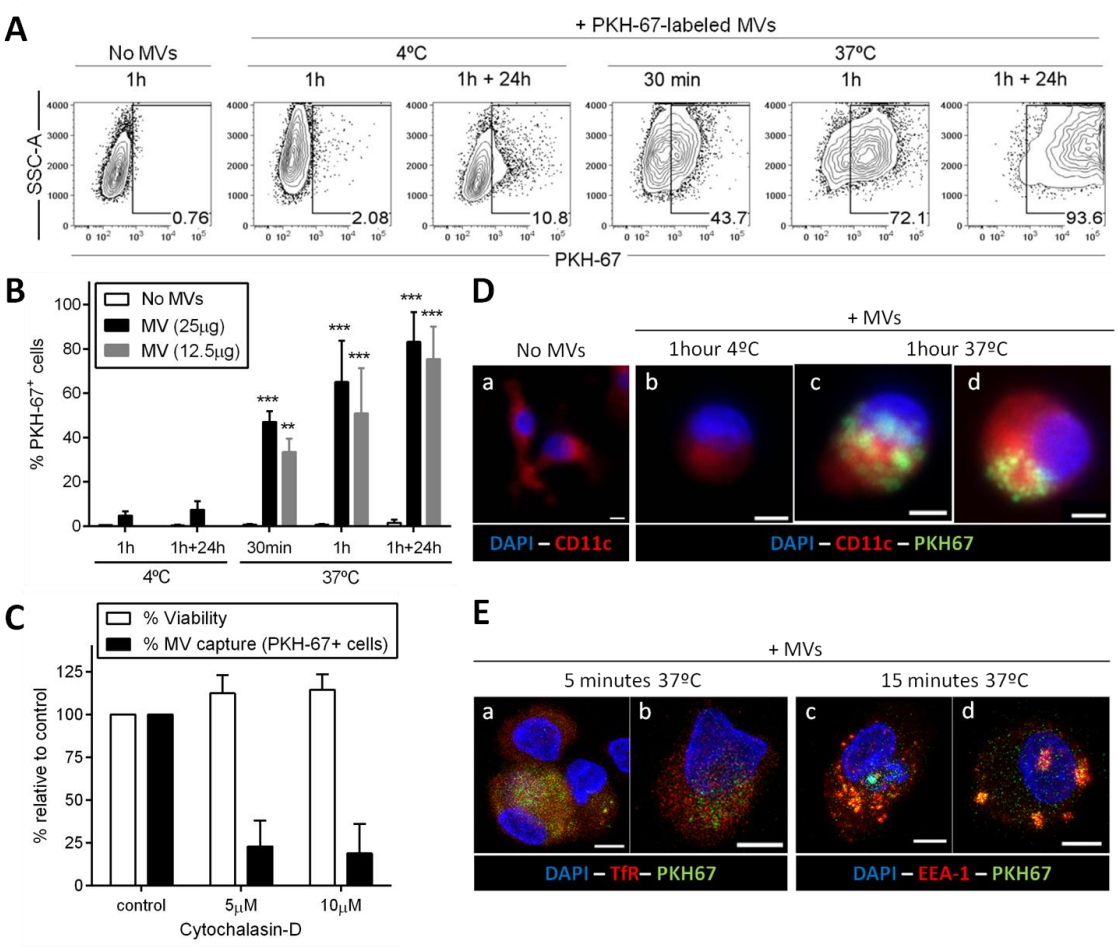
A
+ PKH-67-labeled MVs
No MVs
4ºC
37ºC
1h
1h
1h + 24h
30 min
1h
1h + 24h
SSC-A
0.76
2.08
10.8
43.7
72.1
93.6
PKH-67
B
No MVs
MV (25µg)
MV (12.5µg)
% PKH-67+ cells
1h
1h+24h
30min
1h
1h+24h
4ºC
37ºC
C
% Viability
% MV capture (PKH-67+ cells)
% relative to control
control
5µM
10µM
Cytochalasin-D
D
+ MVs
No MVs
1hour 4ºC
1hour 37ºC
DAPI – CD11c
DAPI – CD11c – PKH67
E
+ MVs
5 minutes 37ºC
15 minutes 37ºC
DAPI – TfR– PKH67
DAPI – EEA-1 – PKH67

Fig. 4

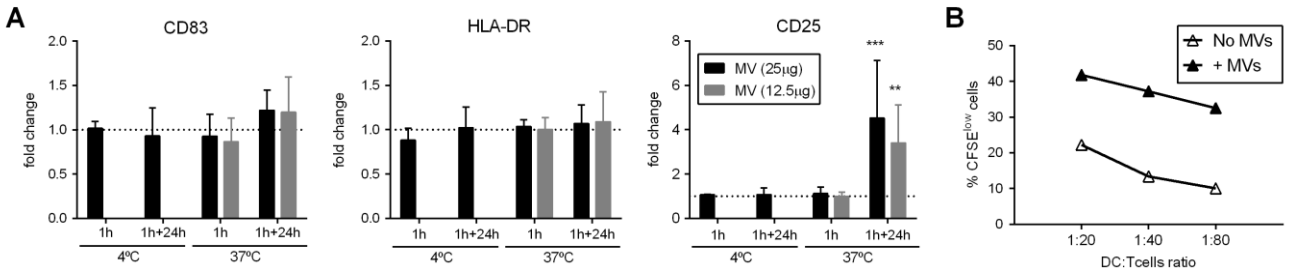
A
CD83
HLA-DR
CD25
fold change
MV (25µg)
MV (12.5µg)
***
**
1h
1h+24h
4ºC
37ºC
B
No MVs
+ MVs
% CFSE low cells
1:20
1:40
1:80
DC:Tcells ratio

Fig. 5

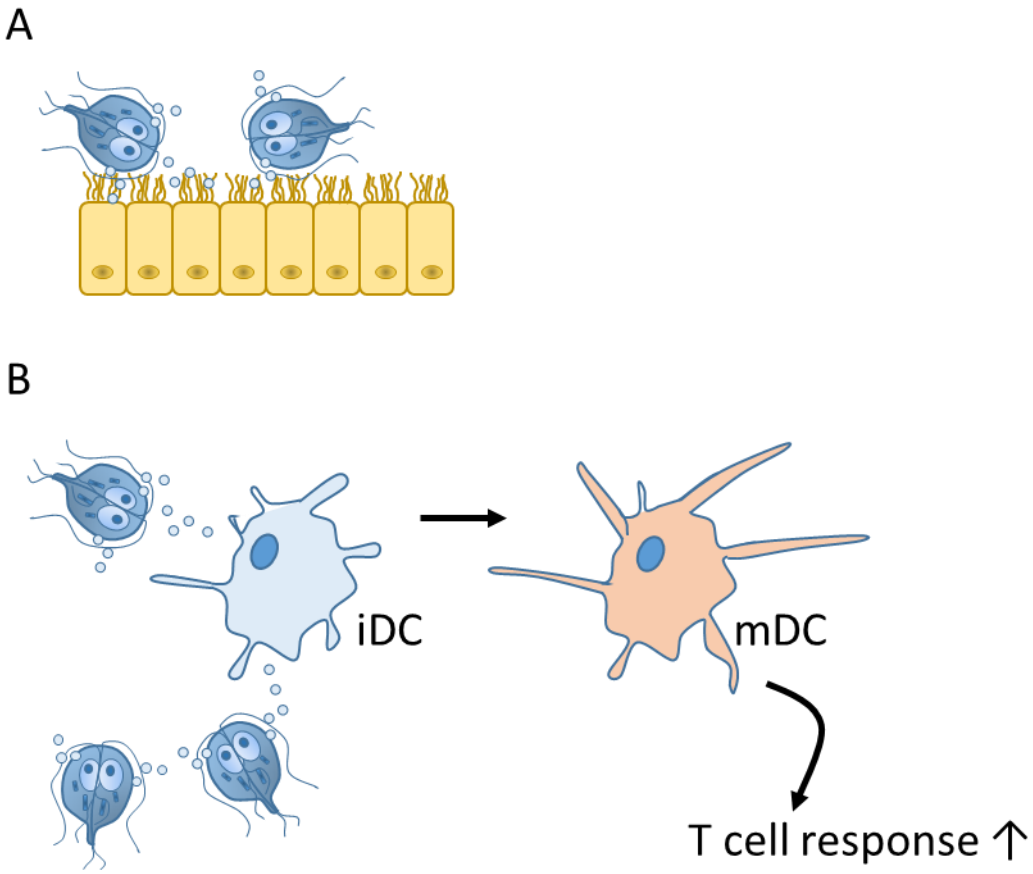

Fig. 6

Table 1- Proteomics analysis of different kind of *Giardia intestinalis* Microvesicles

Accession	Name	Total EmPAI	Homologues EVs
1.2 MVs TROPHOZOITE			
tr|A8BPC0|A8BPC0_GIAIC	Alpha-tubulin	2.79	yes
tr|E2RTT6|E2RTT6_GIAIC	Ornithine carbamoyltransferase	2.42	yes
tr|A8BSP4|A8BSP4_GIAIC	Glyceraldehyde-3-phosphate dehydrogenase	2	yes
tr|E2RU36|E2RU36_GIAIC	Arginine deiminase	2	yes
tr|E2RTN3|E2RTN3_GIAIC	Glucosamine-6-phosphate isomerase	2	yes
RRRRRtr|A8BTS5|A8BTS5_GIAIC	Splicing factor-like protein, putative	1.04	no
RRRRRtr|A8BUK9|A8BUK9_GIAIC	Dynein heavy chain, putative	0.75	yes
tr|A8BS83|A8BS83_GIAIC	rRNA biogenesis protein RRP5	0.14	yes
RRRRRtr|A8BBV7|A8BBV7_GIAIC	Uncharacterized protein	0.08	ND
tr|A8BG55|A8BG55_GIAIC	Uncharacterized protein	0.06	ND
tr|A8BAB7|A8BAB7_GIAIC	Uncharacterized protein	0.05	ND
2.2. MVs CYST 24H			
Cytoskeleton			
tr|A8BEI6|A8BEI6_GIAIC	Beta tubulin	4.86	yes
tr|A8BV70|A8BV70_GIAIC	Actin related protein	2.13	yes
tr|E2RTW1|E2RTW1_GIAIC	Alpha-7.2 giardin	1.44	no
tr|E2RTU4|E2RTU4_GIAIC	Alpha-11 giardin	0.43	no
tr|A8BPC0|A8BPC0_GIAIC	Alpha-tubulin	0.11	yes
tr|A8BER9|A8BER9_GIAIC	Median body protein	0.06	no
Membrane and transport			
tr|A8BN35|A8BN35_GIAIC	Kinesin-like protein	0.14	yes
RRRRRtr|A8BT70|A8BT70_GIAIC	Ciliary dynein heavy chain 11	0.11	yes
RRRRRtr|A8B7D3|A8B7D3_GIAIC	Dynein heavy chain	0.11	yes
tr|E2RU51|E2RU51_GIAIC	TMP52	0.15	no
RRRRRtr|A8BGS8|A8BGS8_GIAIC	WD-repeat membrane protein	0.11	no
tr|A8BUL9|A8BUL9_GIAIC	Cation-transporting ATPase 2, putative	0.06	yes
tr|A8BKH9|A8BKH9_GIAIC	Phospholipid-transporting ATPase IA, putative	0.06	yes
Metabolic enzymes			
tr|E2RTT6|E2RTT6_GIAIC	Ornithine carbamoyltransferase	1.78	yes
RRRRRtr|A8BQI1|A8BQI1_GIAIC	Phosphatidylinositol transfer protein alpha isof	0.21	yes
RRRRRtr|A8B3P9|A8B3P9_GIAIC	Acyl-CoA synthetase	0.02	yes
RRRRRtr|A8B3D3|A8B3D3_GIAIC	Inorganic polyphosphate/ATP-NAD kinase, puta	0.08	no
RRRRRtr|A8BKZ7|A8BKZ7_GIAIC	Protein tyrosine phosphatase-like protein	0.08	yes
tr|A8BYC4|A8BYC4_GIAIC	Peroxiredoxin 1	0.28	yes
tr|A8BVT2|A8BVT2_GIAIC	Midasin ATPase nuclear	0.12	yes
tr|A8BW47|A8BW47_GIAIC	Kinase, NEK	0.1	no
RRRRRtr|A8B8T1|A8B8T1_GIAIC	CDC19 Pyruvate kinase	0.08	yes
Nuclear proteins			
tr|A8BUJ9|A8BUJ9_GIAIC	Histone H4	0.85	yes
RRRRRtr|A8BYH2|A8BYH2_GIAIC	Histone H3	0.06	yes
RRRRRtr|A8BTS5|A8BTS5_GIAIC	Splicing factor-like protein, putative	0.23	no
RRRRRtr|E2RU53|E2RU53_GIAIC	Mre11 endonuclease	0.16	yes
tr|A8B9T6|A8B9T6_GIAIC	Nuclear LIM interactor-interacting factor 1	0.11	no
RRRRRtr|E2RU87|E2RU87_GIAIC	Mlh2-like protein	0.09	no
tr|A8BN96|A8BN96_GIAIC	Reverse transcriptase/endonuclease, putative	0.06	yes
Surface proteins			
tr|A8B1Y1|A8B1Y1_GIAIC	VSP	0.8	no
tr|A8BZM3|A8BZM3_GIAIC	VSP with INR	0.39	no
tr|A8B2E6|A8B2E6_GIAIC	VSP	0.3	no
tr|A8BD73|A8BD73_GIAIC	VSP	0.24	no
Chaperones			
tr|E2RU97|E2RU97_GIAIC	14-3-3 protein	0.56	yes
tr|A8BCR6|A8BCR6_GIAIC	Cytosolic HSP70	0.53	yes
tr|A8BX22|A8BX22_GIAIC	Stress-induced-phosphoprotein 1	0.07	yes
Other			
RRRRRtr|A8BK23|A8BK23_GIAIC	Coiled-coil protein	0.17	no
tr|A8B5R5|A8B5R5_GIAIC	Protein 21.1	0.23	no
RRRRRtr|A8B463|A8B463_GIAIC	Protein 21.1	0.14	no
tr|A8BAF5|A8BAF5_GIAIC	Coiled-coil protein	0.08	no
RRRRRtr|A8BYJ8|A8BYJ8_GIAIC	Mucin-like protein	0.14	yes
tr|A8B4Q1|A8B4Q1_GIAIC	NOD3 protein, putative	0.1	no
tr|A8B4S4|A8B4S4_GIAIC	Retinoic acid induced 17-like protein	0.11	no
tr|A8BNT5|A8BNT5_GIAIC	Ribosomal protein L9	0.12	yes
RRRRRtr|A8BUV6|A8BUV6_GIAIC	Zinc finger domain protein	0.08	no
Unknown			
RRRRRtr|A8BC17|A8BC17_GIAIC	Uncharacterized protein	0.32	
RRRRRtr|A8B9Q6|A8B9Q6_GIAIC	Uncharacterized protein	0.22	
tr|A8BHN6|A8BHN6_GIAIC	Uncharacterized protein	0.21	
tr|A8BQ51|A8BQ51_GIAIC	Uncharacterized protein	0.21	
tr|A8B4W6|A8B4W6_GIAIC	Uncharacterized protein	0.2	
tr|A8BB64|A8BB64_GIAIC	Uncharacterized protein	0.19	
tr|A8BSP2|A8BSP2_GIAIC	Uncharacterized protein	0.18	
tr|D3KGH8|D3KGH8_GIAIC	Uncharacterized protein	0.15	
RRRRRtr|A8B639|A8B639_GIAIC	Uncharacterized protein	0.15	
tr|A8BFN9|A8BFN9_GIAIC	Uncharacterized protein	0.13	
tr|A8B6D8|A8B6D8_GIAIC	Uncharacterized protein	0.12	
tr|D3KI60|D3KI60_GIAIC	Uncharacterized protein	0.11	
tr|A8BMW0|A8BMW0_GIAIC	Uncharacterized protein	0.1	
RRRRRtr|A8BRV4|A8BRV4_GIAIC	Uncharacterized protein	0.1	
RRRRRtr|A8BZ05|A8BZ05_GIAIC	Uncharacterized protein	0.1	
tr|A8BAB7|A8BAB7_GIAIC	Uncharacterized protein	0.1	
tr|A8B688|A8B688_GIAIC	Uncharacterized protein	0.1	